Original Article

The clinical outcome and risk factors analysis of immune checkpoint inhibitor-based treatment in lung adenocarcinoma patients with brain metastases

Juan Zhou[1#], Yinfei Wu[1#], Mengqing Xie[1], Yujia Fang[1], Jing Zhao[1], Sung Yong Lee[2], Yunjoo Im[3], Lingyun Ye[1], Chunxia Su[1]

[1]Department of Oncology, Shanghai Pulmonary Hospital & Thoracic Cancer Institute, Tongji University School of Medicine, Shanghai, China; [2]Division of Pulmonology, Allergy, and Critical Care Medicine, Department of Internal Medicine, Korea University Guro Hospital, Seoul, Republic of Korea; [3]Division of Pulmonary and Critical Care Medicine, Department of Medicine, Samsung Medical Center, Sungkyunkwan University School of Medicine, Seoul, Republic of Korea

Contributions: (I) Conception and design: C Su, L Ye; (II) Administrative support: C Su; (III) Provision of study materials or patients: C Su, J Zhao; (IV) Collection and assembly of data: Y Wu; (V) Data analysis and interpretation: J Zhou, Y Wu, L Ye, C Su; (VI) Manuscript writing: All authors; (VII) Final approval of manuscript: All authors.

[#]These authors contributed equally to this work.

Correspondence to: Chunxia Su; Lingyun Ye. Shanghai Pulmonary Hospital & Thoracic Cancer Institute, Tongji University School of Medicine, No. 507, Zheng Min Road, Yangpu District, Shanghai 200433, China. Email: susu_mail@126.com; yelingyun0712@126.com.

Background: The data about efficacy of immunotherapy for non-small cell lung cancer with brain metastases (BMs) from real-word settings are controversial. This real-word study is aimed to evaluate the clinical outcome of immune checkpoint inhibitor (ICI)-based treatment in lung adenocarcinoma patients with brain metastases (BMs) and explore potential risk factors, with a focus on the spatial distribution of BMs as previous studies suggested spatial heterogeneity on the brain immune microenvironment.

Methods: Advanced lung adenocarcinoma patients with non-oncogene-addicted, who received ICI monotherapy or plus chemotherapy, were enrolled. Efficacy was assessed by Response Evaluation Criteria in Solid Tumors version 1.1. Intergroup comparisons were performed using Pearson's χ^2 or Fisher's exact tests for categorical variables. The progression-free survival (PFS) was estimated using Kaplan-Meier method and compared using log-rank test. Cox proportional hazards model was used for multivariate analyses. Peripheral blood was collected from 15 patients with BMs. Tumor-derived exosomes in plasma were isolated by size exclusion chromatography and the cDNA library preparations for miRNA were sequenced on an Illumina Hiseq platform. Differentially expressed genes in the Kyoto Encyclopedia of Genes and Genomes (KEGG) pathways were analyzed.

Results: A total of 198 patients were enrolled and brain metastasis occurred in 20.7% patients (N=41). Compared with patients without BMs, those with BMs had a comparable objective response rate (ORR; 29.3% *vs.* 43.9%; P=0.089), a lower disease control rate (DCR; 58.5% *vs.* 78.3%; P=0.01), and a shorter PFS (3.6 *vs.* 8.6 months; P=0.069). For patients with BMs, factors, including the presence of neurological symptoms, the treatment of intracranial radiotherapy, and the combination of ICI with chemotherapy, had no impact on PFS, whereas cerebellum metastasis was significantly associated with shorter PFS (2.8 *vs.* 13.8 months, P=0.007). Six upregulated miRNAs were identified in patients with cerebellum metastases (N=8) compared with those without (N=7). The enrichment of differentially expression genes in the KEGG pathways indicated upregulated sulfur metabolism pathway in patients with cerebellum metastases.

Conclusions: For lung adenocarcinoma patients, those with BMs have inferior response to ICI-based treatment, but not significantly, and cerebellum metastasis is an independent risk factor with poor outcome for such patients, might attributing to the upregulated sulfur metabolism.

Keywords: Lung adenocarcinoma; immune checkpoint inhibitor (ICI); cerebellum metastasis

Submitted Jan 21, 2022. Accepted for publication Apr 20, 2022.
doi: 10.21037/tlcr-22-260
View this article at: https://dx.doi.org/10.21037/tlcr-22-260

Introduction

The brain is one of the most common sites of distant metastasis for non-small cell lung cancer (NSCLC) (1). With improvements in systemic therapy, the longer survival of patients also translates to increased incidence of brain metastasis (BM). A large study, involving 457,481 patients with NSCLC, reported that BM was detected in 26% of patients with stage IV disease at presentation, and adenocarcinoma histology was significantly associated with the presence of BM compared with squamous cell lung cancer (26.8% *vs.* 15.9%, odds ratio 2.93) (2). BM is traditionally considered a negative factor for treatment efficacy and survival prognosis, but unprecedented achievements in the use of immune checkpoint inhibitor (ICI) in lung cancer patients have propelled this issue into a new clinical practice setting.

ICI was believed to be ineffective for intracranial lesions since brain was thought as an immune-privileged site due to the blood-brain barrier. In addition, the large molecular size of the antibody reduced intracerebral drug availability (3). However, retrospective analysis of clinical trials [KeyNote 024 (4) and KeyNote 189 (5)] suggested that NSCLC patients with brain metastases (BMs) could derive survival benefits from ICI-based treatment compared with chemotherapy. A pooled analysis (6) of KeyNote-001, -010, -024, and -042 studies also indicated that for patients with high programmed cell death ligand-1 (PD-L1) expression, the advantages of overall survival (OS) gained from pembrolizumab over chemotherapy were comparable between patients with and without BMs [hazard ratio (HR) 0.83 versus 0.78]. Nevertheless, the population from clinical trials has been selected by rigorous criteria, much differing from that in real-word practice. Clinically, the presence of neurological symptoms, the use of glucocorticoid and the treatment of intracranial radiotherapy are important for the prognosis of patients with BMs. Some studies have proved that the treatment of glucocorticoid or intracranial radiotherapy had influences on activity of ICI (7,8). But, in fact, only 6.2–17.5% of the patients enrolled in the pivotal NSCLC ICI trials had asymptomatic or previously treated or stable BMs, and none of them allowed patients with symptomatic or untreated BMs (9). Recently, a prospective phase II study (10) examined the efficacy of ICI in advanced NSCLC patients with untreated BMs and showed an intracranial response of 29.7%, but it still required patients be no neurologic symptomatic. The data from real-word practice about efficacy of ICI on patients with BMs remain limited and controversial. For example, a subgroup analysis from Qiao *et al.*'s study (11) indicated that NSCLC patients with BMs had significantly shorter progression-free survival (PFS) and OS than those without, whereas another real-word study by Sun *et al.* suggested a comparable objective response rate (ORR), PFS, and OS between patients with and without BMs (12). Therefore, further studies are needed to better clarify the efficacy of ICI for NSCLC patients with BMs and to identify the relevant risk factors in a clinical practice setting.

In addition, the reported risk factors affecting the prognosis of NSCLC patients with BMs include age, Karnofsky Performance Status, extracranial metastases, the number of BMs, molecular subtype, the method of intracranial radiotherapy, carcinoembryonic antigen levels, and so on (13-17), however, there is no study on the correlation between the location of BMs and prognosis. We notice that the tumor microenvironment in BMs is organ-specific as there are some specialized resident immune cells, like astrocytes and microglia that are proved to be crucial in promoting tumor progression and immune evasion in NSCLC BMs (18,19). Previous studies suggested that these cells were much heterogeneous in their morphological and functional properties based on their different spatiotemporal distribution (20,21), existing influences on tumor microenvironment and malignant progression (22). Thus, we speculated that regional heterogeneity of the brain microenvironment might lead to different responses of metastatic tumors to immunotherapy.

Collectively, this real-word study is aimed to evaluate the efficacy and clinical outcome of ICI-based treatment in lung adenocarcinoma patients with BMs and to explore the potential risk factors that affect those patients' outcome, with a special focus on the spatial distribution of BMs. We present the following article in accordance with the STROBE reporting checklist (available at https://tlcr.amegroups.com/article/view/10.21037/tlcr-22-260/rc).

Methods

Patients

Patients with advanced lung adenocarcinoma who were admitted to the Shanghai Pulmonary Hospital between July 2018 and November 2020 were enrolled in this study. The following inclusion criteria were applied: (I) adenocarcinoma diagnosis confirmed by pathology; (II) stage IV disease according to the eighth edition of the TNM classification for lung cancer; (III) measurable lesions according to the Response Evaluation Criteria in Solid Tumors version 1.1 (RECIST v1.1); and (IV) received ICI-based treatment (ICI monotherapy or ICI plus chemotherapy). The exclusion criteria included the followings: (I) patients with oncogene-addicted, including epidermal growth factor receptor (EGFR), anaplastic lymphoma kinase (ALK), and c-ros oncogene 1, receptor tyrosine kinase (ROS1); (II) patient with insufficient data or follow-up time <3 months; (III) patients who had received other immunotherapy, including but not limited to vaccines and adoptive cellular immunotherapy; (IV) presence of active multiple primary malignancies; and (V) patients who was receiving intensive immunosuppressive agents. The patients were followed up by telephone consultation. The study was conducted in accordance with the Declaration of Helsinki (as revised in 2013). The study was approved by the ethics committee of Shanghai Pulmonary Hospital, Tongji University (No. 201907-0375). Informed consents were obtained from patients whose peripheral blood was collected for further exosome analysis and the other patients were informed by telephone because of the retrospective nature.

Efficacy assessment

Efficacy was assessed according to the standard of RECIST v1.1. An intracranial response was assessed by brain magnetic resonance imaging (MRI), using modified RECIST that defined target central nerve system lesions as lesion ≥5 mm in maximum diameter, with up to five lesions in patients with multiple lesions . The ORR was the proportion of patients who had complete response (CR) or partial response (PR) to treatment. The disease control rate (DCR) was the proportion of patients who had CR, PR, or stable disease (SD) to treatment. The PFS was defined as the interval from the initiation of ICI-based therapy to first RECIST v1.1-defined progression disease (PD) or death from any cause, whichever occurred first. If patient was not followed with PD, the data would be censored at the time of last chest computed tomography. The data of PD-L1 expression were collected which was evaluated by immunohistochemical (IHC) method using E1L3N or 22C3 antibody.

Isolation and analysis of tumor-derived exosome

Exosomes were isolated by size exclusion chromatography (SEC) according to the manufacturer's instructions (23). Briefly, 1 mL of 0.8 μm-filtered blood plasma was diluted 1.5-fold with phosphate buffered saline (PBS) and further purified using Exosupur® columns (Echobiotech, China). Next, the samples were eluted with 0.1 M PBS and 2 mL eluate fractions were collected. Fractions were concentrated to 200 μL using 100 kDa molecular weight cut-off Amicon® Ultra spin filters (Merck, Germany).

Total RNA was extracted and purified from plasma exosome using miRNeasy Serum/Plasma Advanced Kit (Qiagen, cat. No. 217204) according to the kit instruction. RNA concentration and purity were evaluated using the RNA Nano 6000 Assay Kit of the Agilent Bioanalyzer 2100 System (Agilent Technologies, CA, USA). For small RNA libraries, a total amount of 1–500 ng. RNA per sample was used for sample preparations. QIAseq miRNA Library Kit (Qiagen, Frederick, MD) was used to generate sequencing libraries and index codes were added to each sample. Reverse transcription (RT) primers with unique molecular indices (UMIs) were introduced to analyze the quantification of miRNA expressions during cDNA synthesis and PCR amplification. And then, library quality was evaluated on the Agilent Bioanalyzer 2100 and further verified by qPCR. acBot Cluster Generation System was used to cluster the index-coded samples through TruSeq PE Cluster Kitv3-cBot-HS (Illumina, San Diego, CA, USA) according to the instructions. At last, the prepared library was sequenced on an Illumina Hiseq platform to generate paired-end reads.

Firstly raw data in fastq format were processed using in-house perl scripts to filter out reads containing adapter, reads containing ploy-N and low-quality reads. The obtained clean data were used to calculate Q20, Q30, GC-content and sequence duplication level. All the downstream analyses were based on these high quality clean data. Paired-end clean reads were aligned to the reference genome-GRCh38 using TopHat2/Bowtie2 (24). Mapped reads were used for the Quantification of gene expression level and Differential expression analysis. Bowtie tools soft was used

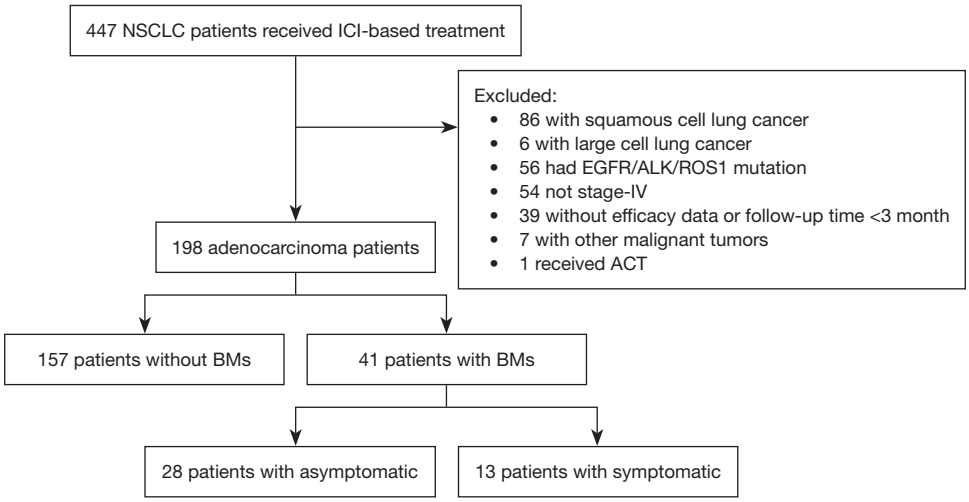

Figure 1 Flowchart of the study. NSCLC, non-small cell lung cancer; ICI, immune checkpoint inhibitor; EGFR, epidermal growth factor receptor; ALK, anaplastic lymphoma kinase; ROS1, c-ros oncogene 1, receptor tyrosine kinase; ACT, adoptive cell therapy; BMs, brain metastases.

to make sequence alignment for the clean reads respectively with Silva database, GtRNAdb database, Rfam database and Repbase database, to filter out ribosomal RNA (rRNA), transfer RNA (tRNA), small nuclear RNA (snRNA), small nucleolar RNA (snoRNA) and other ncRNA and repeats. Known miRNAs were detected and new miRNAs were predicted in the remaining reads by sequencing alignment with miRbase and Human Genome (GRCh38), respectively. Expression matrix of quantified UMI counts of miRNAs was normalized to counts per million (CPM) and calculated to relative log expression via the EdgeR package.

The Kyoto Encyclopedia of Genes and Genomes (KEGG) (25) is a database resource that is used to analyze high-level functions and utilities of the biological system including from molecular-level information, especially large-scale molecular datasets generated from genome sequencing or other high-throughput experimental technologies (http://www.genome.jp/kegg/). The KOBAS (26) software was used to assess the statistical enrichment of the differentially expressed genes in the KEGG pathways.

Statistical analysis

The SPSS software (version 22.0) was used for statistical analyses. Differential expression analysis of two groups was performed using the Mann-Whitney U test with cutoff FPKM >5, P value <0.05, and fold change >1.5 (the FPKM represented the fragments per kilo-base of exon per million fragments mapped, and is calculated based on the length of the fragments and read counts mapped to this fragment). Intergroup comparisons were performed using the Pearson's χ^2 or Fisher's exact tests for categorical variables. The PFS and OS were estimated using the Kaplan-Meier method and compared using log-rank test in univariate analyses. Factors with P value <0.1 in the univariate analysis were included for multivariate analysis using the Cox proportional hazards model, which was also used to calculate the HR and corresponding 95% confidence interval (CI). A two-sided P value <0.05 was considered significant.

Results

Characteristics of the study population

A total of 198 patients with advanced lung adenocarcinoma were enrolled into this study and BM was detected in 20.7% of patients (N=41; *Figure 1*). Of the 41 patients, 13 had neurological symptoms before ICI-based treatment, but only 2 patients were administered corticosteroid. Brain MRI was performed within 6 weeks prior to ICI-based treatment in 36 (87.8%) patients. Twenty-one (51.2%) patients had received intracranial radiotherapy, 13 of whom received concurrent intracranial radiotherapy with ICI-based treatment, which was defined as less than 3 months between the initial of ICI and intracranial radiotherapy. Majority of patients (63.1%) received ICI plus chemotherapy. Notably, only 6 patients received ICI monotherapy as first-line

treatment, while 67 patients were treated ICI monotherapy as posterior-line therapy. Clinical characteristics before ICI-based treatment were compared between patients with and without BMs (*Table 1*). Patients with BMs had poorer Eastern Cooperative Oncology Group (ECOG) score (P<0.001) and more extracranial metastases (ECM) (P<0.001) compared to those without. Other characteristics such as age, gender, smoking history, gene type, and PD-L1 expression were balanced between the two groups.

The outcomes of ICI-based treatment

The median follow-up time was 31.7 months. In total, progression events occurred in 32 (78%) patients with BMs and 125 (79.6%) patients without BMs. Patients with and without BMs had comparable ORR (29.3% *vs.* 43.9%; P=0.089). However, patients with BMs showed a lower DCR (58.5% *vs.* 78.3%; P=0.01) and shorter a PFS (3.6 *vs.* 8.6 months; P=0.069; HR =1.428; 95% CI: 0.924 to 2.207; *Figure 2A*,*2B*). Intracranial efficacy was assessed in 31 patients and the majority had concordant responses to ICI-based treatment between intracranial lesion and primary lung lesion (77.4%; *Figure 2C*), with an intracranial ORR of 35.5% and an intracranial DCR of 71.0%.

The analysis of risk factors

For patients with BMs, those who presented with neurological symptoms had similar PFS to asymptomatic patients (3.0 *vs.* 4.4 months; P=0.553; Figure S1A). There was also no difference in PFS between patients who received intracranial radiotherapy and those who did not (Figure S1B). Patients who received combination therapy appeared to have superior PFS compared to patient who received ICI monotherapy (6.3 *vs.* 2.9 months; P=0.069; Figure S1C), however, it should be noted that there was only 1 patient who received first-line treatment in the monotherapy group, whereas 48.0% in the combination group. Further analysis in patients who received posterior-line ICI-based treatment suggested that there was no significant difference in PFS between the combination and monotherapy groups (Figure S1D).

The progression of intracranial lesion was confirmed in 17 patients (41.5%) and the median intracranial PFS (icPFS) of patients with BMs was 12.9 month (Figure S2A). No difference in median icPFS was observed between patients with symptomatic and asymptomatic BMs (Figure S2B). Neither combination therapy nor intracranial radiotherapy was associated with intracranial survival (Figure S2C,S2D). In addition, the progression of intracranial lesion was more common in patients with BMs than in patients without BMs (40.6% *vs.* 4.8%; P<0.001). The progression patterns of these two groups are shown in Figure S3.

The impact of BMs' spatial distribution on ICI-based treatment outcomes

To investigate the impact of different regions involved in BMs on the clinical outcome of ICI-based treatment, five functional lobes were assessed, including frontal, parietal, temporal, occipital, and cerebellum. The distribution of BMs for patients with baseline brain MRI is showed in *Figure 3A*. The most frequency site of BM was the frontal lobe, followed by the parietal, temporal, occipital, and cerebellum. The impacts of each region involvement on the PFS are shown in *Figure 3B-3F*. The results suggested that only cerebellum metastasis was significantly associated with shorter PFS of ICI-based therapy (2.8 *vs.* 13.8 months; P=0.007). However, it was noted that cerebellum metastasis was often accompanied with extensive BMs. Among the 15 patients with cerebellum metastases, 7 (46.7%) patients had concurrent metastases in all the above five regions, and the median PFS for these patients was significantly shorter than those without extensive metastases (less than five functional regions) (2.8 *vs.* 5.6 months; P=0.021; *Figure 3G*). Analysis of baseline characteristics also suggested that the number of BMs was greater in patients with cerebellum metastases than that in patients without (P=0.001; *Table 2*). Nevertheless, when these 7 patients with extensive BMs were excluded, the median PFS of the remaining 8 patients was still 2.8 months. Specifically, PFS of all these patients were shorter than 6 months, except for 1 patient who had a PFS of 13.3 months. Univariate and multivariate analyses demonstrated that cerebellum metastasis was an independent risk factor for PFS of ICI-based treatment (Table S1). As for the impact of different regions on icPFS, the results also suggested that cerebellum metastasis was the only risk factor (Figure S4A-S4F). Together, these data suggested that cerebellum metastasis is a poor factor for the clinical outcome of ICI-based treatment in lung adenocarcinoma patients with BMs.

The differences in the tumor-derived exosomes between patients with and without cerebellum metastases

We had collected plasma samples from 15 patients with

Table 1 Baseline characteristics of all patients

Characteristics	Total (n=198), n (%)	Without BMs (n=157), n (%)	With BMs (n=41), n (%)	P value
Age, years				0.073[#1]
<50	34 (17.2)	22 (14.0)	12 (29.3)	
50–60	73 (36.8)	60 (38.2)	13 (31.7)	
>60	91 (46.0)	75 (47.8)	16 (39.0)	
Sex				0.846[#1]
Male	143 (72.2)	114 (72.6)	29 (70.7)	
Female	55 (27.8)	43 (27.4)	12 (29.3)	
Smoking				0.100[#1]
No/light	126 (63.6)	95 (60.5)	31 (75.6)	
Heavy[‡]	72 (36.3)	62 (39.5)	10 (24.4)	
ECOG				<0.001[#2]
0–1	181 (91.4)	150 (95.5)	31 (75.6)	
2–3	17 (8.6)	7 (4.5)	10 (24.4)	
Gene mutation				0.450[#2]
Wild type	150 (75.8)	120 (76.4)	30 (73.2)	
KRAS	29 (14.6)	24 (15.3)	5 (12.2)	
Other[§]	19 (9.6)	13 (8.3)	6 (14.6)	
PD-L1*				0.563[#2]
≥50%	12 (21.1)	9 (18.8)	3 (33.3)	
1–49%	16 (28.1)	13 (27.1)	3 (33.3)	
Negative	29 (50.9)	26 (54.2)	3 (33.3)	
Unknown	141 (71.2)	109 (69.4)	32 (78.0)	
ECM				<0.001[#1]
Present	84 (42.4)	78 (49.7)	36 (87.8)	
Absent	114 (57.6)	79 (50.3)	5 (12.2)	
ICI line				0.370[#1]
1	76 (38.4)	63 (40.1)	13 (31.7)	
≥2	122 (61.6)	94 (59.9)	28 (68.3)	
ICI drug				0.707[#2]
Pembrolizumab	57 (28.8)	42 (26.8)	15 (36.6)	
Nivolumab	25 (12.6)	19 (12.1)	6 (14.6)	
Camrelizumab	71 (35.9)	59 (37.6)	12 (29.3)	
Sintilimab	19 (9.6)	16 (10.2)	3 (7.3)	
Tislelizumab	13 (6.6)	10 (6.4)	3 (7.3)	
Toripalimab	10 (5.1)	9 (5.7)	1 (2.4)	

Table 1 *(continued)*

Table 1 *(continued)*

Characteristics	Total (n=198), n (%)	Without BMs (n=157), n (%)	With BMs (n=41), n (%)	P value
Others	3 (1.5)	2 (1.2)	1 (2.4)	
Treatment regimen				0.856[#1]
Mono	73 (36.9)	57 (36.3)	16 (39.0)	
Combination	125 (63.1)	100 (63.7)	25 (61.0)	

[†], heavy smoking was defined as the package*year ≥30; [§], other gene mutations included BRAF V600E (n=4), Her-2 mutation (n=6), Her-2 amplification (n=2), RET fusion (n=4), TP53 mutation (n=2), MET mutation (n=1); *, antibodies for testing PD-L1 expression include E1L3N and 22C3. [#1]: using Pearson's χ^2 for variables that have no cell with expected count less than 5; [#2]: using Fisher's exact for variables that have ≥1 cells with expected count less than 5. BMs, brain metastases; ECOG Eastern Cooperative Oncology Group; PD-L1, programmed cell death ligand 1; ECM, extracranial metastases; ICI, immune checkpoint inhibitor; Mono, monotherapy.

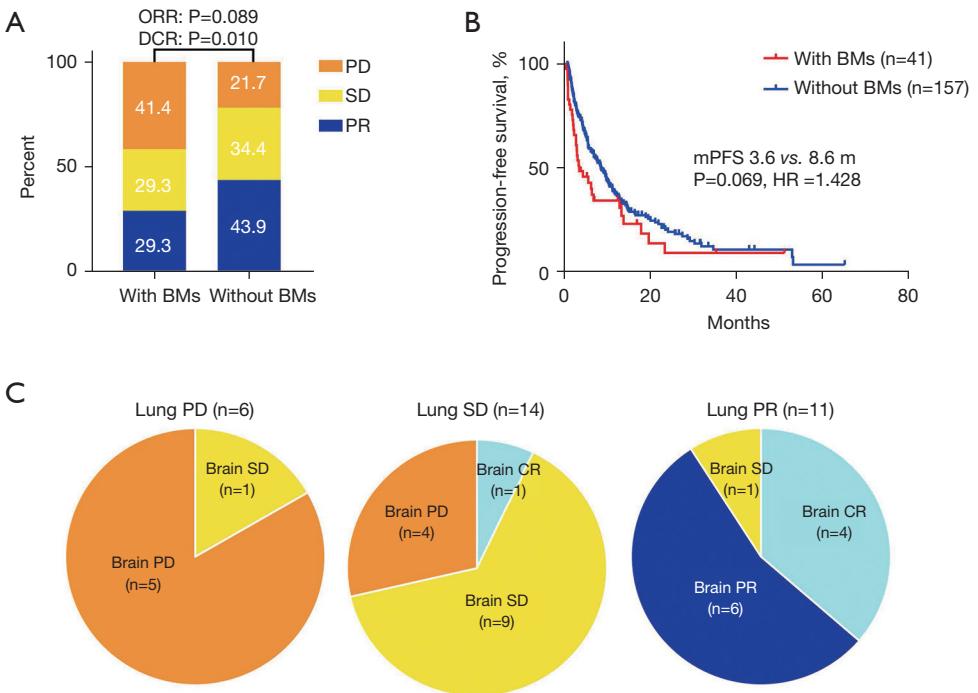

Figure 2 Clinical outcomes of ICI-based therapy comparison in patients with or without BMs. Response (A) and PFS (B) comparison. Responses in primary lung lesion and paired intracranial lesion (C). ORR, objective response rate; DCR, disease control rate; PD, progression disease; SD, stable disease; PR, partial response; CR, complete response; ICI, immune checkpoint inhibitor; BMs, brain metastases; PFS, progression-free survival; mPFS, median PFS.

BMs, including 8 patients accompany with cerebellum metastases and 7 patients without. Considering that the important role of tumor-derived exosomes both in regulating immune cells (27) and promoting BM (28), we performed miRNA sequencing from the tumor-derived exosomes in plasma to explore the underlying mechanisms of the different prognosis between the two groups. In total, 1,113 miRNAs were detected, of which 1,081 were known and 52 were newly predicted. Differential expression analysis revealed that 6 upregulated miRNAs were expressed in patients with cerebellum metastases, including hsa-miRNA-331-5p, -542-5p, 26a-2-3p, -99a-3p, -184, and -3065-5p (*Figure 4A,4B*). A total of 29 target genes were predicted from these miRNAs (Table S2). The enrichment

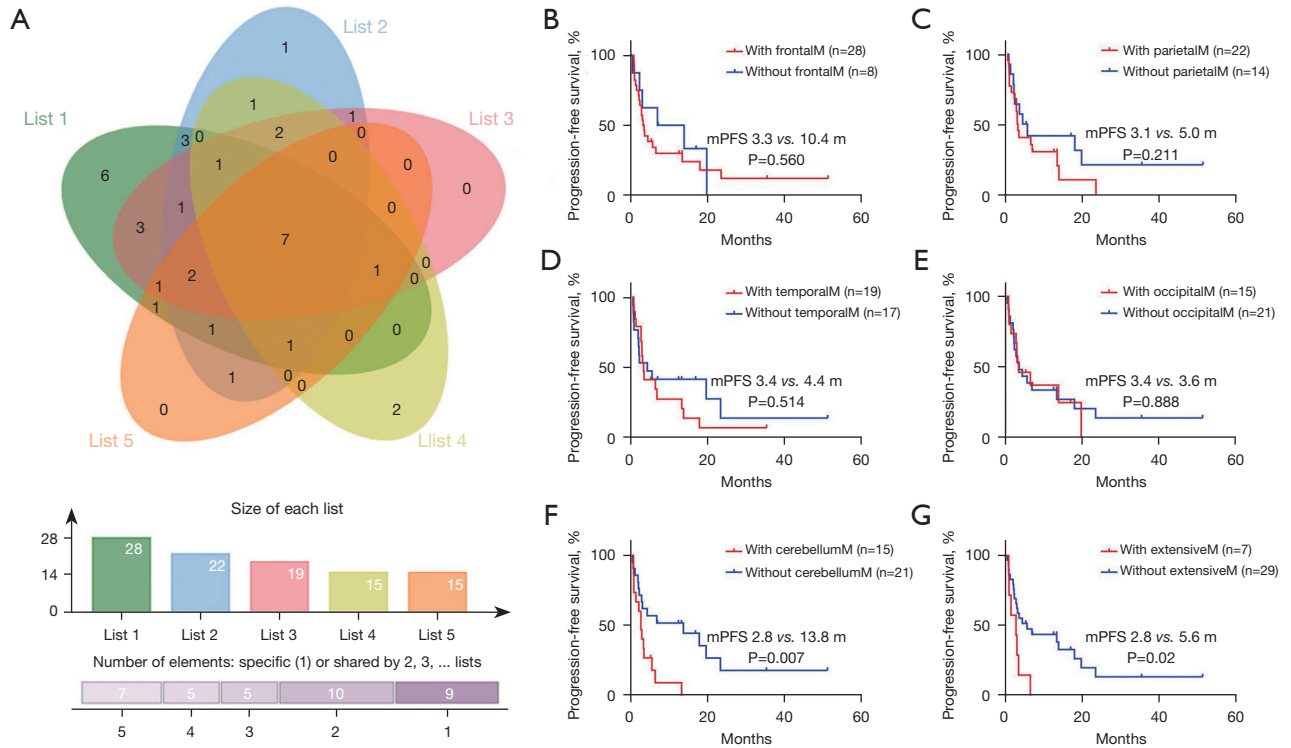

Figure 3 The region distribution of BMs for patients with baseline brain MRI (A). PFS comparison between patients with or without different region metastases: frontal lobe (B), parietal lobe (C), temporal lobe (D), occipital lobe (E), cerebellum (F), and concurrent the above five regions (G). M, metastases; BMs, brain metastases; MRI, magnetic resonance imaging; PFS, progression-free survival; mPFS, median PFS.

of differential expression genes in KEGG pathways analysis indicated that the sulfur metabolism pathway was the most significantly upregulated pathway in patients with cerebellum metastases (*Figure 4C*).

Discussion

The efficacy of ICI on NSCLC patients with BMs remains controversial, since such patients are often excluded from clinical trials, or only patients with stable BMs are selected. The study from Hendriks *et al.* included a cohort of less-selected NSCLC patients with BMs and demonstrated that such patients had shorter PFS and OS, similar overall ORR, and lower DCR compared to patients without BMs (7). This agrees with our current study demonstrating that patients with BMs had similar PFS and ORR, and higher DCR compared to patients without BMs. However, it worth noting that the former study excluded patients treated with anti-PD-1 inhibitor plus chemotherapy, whereas about 63% of our cohort consisted of such patients. The different response between BMs and primary lung lesion is another focus of concern regarding immunotherapy in NSCLC. The study by Kim *et al.* (29) suggested that BMs are poorly responsive to anti-PD-1 therapy. Our present study showed major coincident responses of intracranial lesion and lung lesion, though discordant responses existed in minority of patients.

The heterogeneity of functional areas in the brain has been observed from several aspects. Gryglewski *et al.* discovered that gene expression exhibited a high spatial dependence among the cortical surface, subcortical regions, and cerebellum (30). Kleinridders and colleagues found significant regional differences in glucose metabolism between the thalamus and the cortex (31). However, to date, whether the heterogeneity across different regions of brain affects the intracranial efficacy of ICI-based therapy remains to be elucidated. To the best of our knowledge, the present study is the first to report that cerebellum metastasis is associated with poorer outcome after ICI-based therapy in lung adenocarcinoma patients with BMs. This may be caused by a more suppressive immune microenvironment in cerebellum, as suggested by Ayata *et al.*, who demonstrated that microglia in cerebellum exhibited higher clearance

Table 2 Baseline characteristics of patients with BMs

Characteristics	Total (n=41), n (%)	Without cerebellum M (n=21), n (%)	With cerebellum M (n=20), n (%)	P value
Age, years				0.361[#1]
<50	12 (29.3)	4 (19.0)	8 (40.0)	
50–60	13 (31.7)	8 (38.1)	5 (25.0)	
>60	16 (39.0)	9 (42.9)	7 (35.0)	
Sex				0.431[#1]
Male	29 (70.7)	16 (76.2)	13 (65.0)	
Female	12 (29.3)	5 (23.8)	7 (35.0)	
Smoking[†]				1.000[#2]
No/light	31 (75.6)	16 (76.2)	15 (75.0)	
Heavy	10 (26.3)	5 (23.8)	5 (25.0)	
ECOG				1.000[#2]
0–1	31 (75.6)	16 (76.2)	15 (75.0)	
2–3	10 (24.4)	5 (23.8)	5 (25.0)	
ECM				1.000[#2]
Present	10 (24.4)	5 (23.8)	5 (25.0)	
Absent	31 (75.6)	16 (76.2)	15 (75.0)	
No. of BMs				0.002[#2]
<5	22 (53.7)	16 (76.2)	6 (30.0)	
5–10	13 (31.7)	5 (23.8)	8 (40.0)	
>10	6 (14.6)	0 (0.0)	6 (30.0)	
DS-GPA				0.342[#2]
0–1.0	7 (17.1)	2 (9.5)	5 (25.0)	
1.5–2.0	25 (61.0)	15 (71.4)	10 (50.0)	
2.5–3.0	8 (19.5)	4 (19.0)	4 (20.0)	
3.5–4.0	1 (2.4)	0 (0.0)	1 (2.4)	
Neurological symptom				0.265[#1]
Yes	13 (31.7)	5 (23.8)	8 (40.0)	
No	28 (68.3)	16 (76.2)	12 (60.0)	
Intracranial radiotherapy				0.085[#1]
Yes	21 (51.2)	8 (38.1)	13 (65.0)	
No	20 (48.8)	13 (61.9)	7 (35.0)	
ICI line				0.368[#1]
1	13 (31.7)	8 (38.1)	5 (25.0)	
≥2	28 (68.3)	13 (61.9)	15 (75.0)	
Treatment regimen				0.444[#1]
Mono	16 (39.0)	7 (33.3)	9 (45.0)	
Combination	25 (61.0)	14 (66.7)	11 (55.0)	

[†], heavy smoking was defined as the package*year ≥30. [#1]: using Pearson's χ^2 for variables that have no cell with expected count less than 5; [#2]: using Fisher's exact for variables that have ≥1 cells with expected count less than 5. BMs, brain metastases; ECOG, Eastern Cooperative Oncology Group; PD-L1 programmed cell death ligand-1; ECM, extracranial metastases; DS-GPA, diagnosis-specific graded prognostic assessment; ICI, immune checkpoint inhibitor; Mono, monotherapy; M, metastasis.

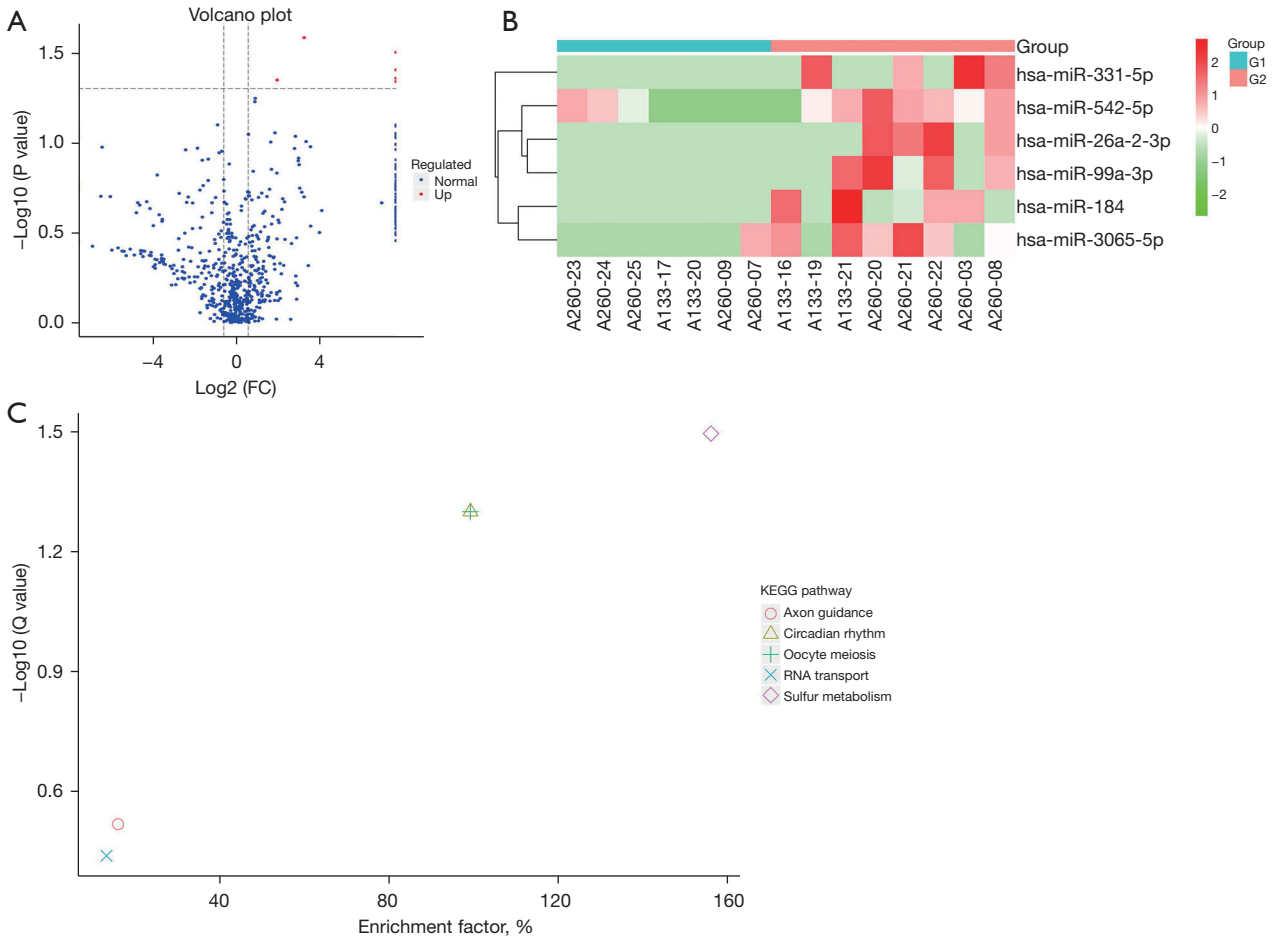

Figure 4 Differential analysis on miRNA of tumor-derived exosomes extracted from patients with or without cerebellum metastases (A,B). (C) Result of the KEGG pathways analysis based on the differential expressed miRNA. KEGG, Kyoto Encyclopedia of Genes and Genomes.

activity than that in the striatal or cortical (32). In addition, it was noted that patients with cerebellum metastases were inclined to develop extensive BMs, suggestive of a more invasive tumor. This newly identified risk factor may be partially responsible for the heterogeneous outcome of NSCLC patients with BMs, which may explain, at least to some extent, the conflicting data regarding the efficacy of CI-based therapy in such patients.

Exosomes derived from tumor cells are now known to play a crucial role in metastatic brain tumors (28,33-35). Fong *et al.* (36) showed that the level of miR-122 secreted by breast cancer cells into the circulation was associated with brain and lung metastasis. In our study, by performing miRNA-sequencing on exosomes extracted from the peripheral blood of patients, 6 upregulated miRNAs were identified in patients with cerebellum metastases compared to those without, suggesting differences in tumor biological characteristics. Moreover, the KEGG enrichment pathway analysis demonstrated that patients with cerebellum metastases had upregulated sulfur metabolism. Metabolic reprogramming, which is now well documented to be related to immune response (37,38), is also observed in BMs (39-41). However, it remains unknown whether metabolic dysregulation in BMs can affect the response to ICI. Indeed, the results in the present study suggested that sulfur metabolism was upregulated in patients with cerebellum metastases and might correlate with the poor outcome of ICI treatment. Previous studies have reported that sulfur and its intermediate metabolites are important for cellular metabolism, since they are not only required in oxidation/reduction reactions, but also mediate inter- and intracellular signaling, and facilitate the epigenetic regulation of gene expression (42,43). The dysregulation of sulfur metabolism may contribute to tumorigenesis and progress (44).

Interestingly, sulfurous compounds are also essential for sustaining neurological functions. For example, disturbances in the hydrogen sulfide and trans-sulfuration pathways have been implicated in neurodegenerative disorders such as Alzheimer's disease and Parkinson disease (45). Therefore, upregulated sulfur metabolism in patients with cerebellum metastases may lead to more aggressiveness tumors, which may also be related to the neurological symptoms commonly observed in such patients. However, the results of our KEGG analysis are limited by the sample size and the nature of this method, and further cell and animal studies are warranted to verify the role of exosome miRNA and sulfur metabolism in cerebellum metastasis.

In addition, the circadian rhythm and oocyte meiosis pathways were also upregulated in patients with cerebellum metastases as showed in KEGG analysis. Because the cerebellum contains a circadian clock, generating internal temporal signals, we firstly thought that the circadian rhythm pathway upregulation was attributed to occupied effect of metastatic brain tumors. Zhang *et al.* also found hyperactivated circadian rhythm pathway in lower grade glioma (46). However, many extracranial tumors, such like lung, breast, colorectal cancer, and head and neck squamous cell carcinoma, could also mediate the disruption of circadian rhythm, which influenced cancer development by regulating tumor cell apoptosis, immune infiltration, and tumor cell-host interactions (47-51). But the role of dysregulated circadian rhythms in metastatic brain tumor development and its immune response remains unclear and further studies are in needed. As for oocyte meiosis, although its enrichment was reported in some researches about lung cancer (52,53), further function and mechanism studies are lacked. The role of oocyte meiosis in BM or cerebellum is rarely studied, either.

Biomarkers are urgently needed to predict the efficacy of ICI-based therapy for NSCLC patients, especially those with BMs. Thus far, only PD-L1 expression has been shown to be associated with the clinical outcome of patients with BMs when treated with ICI monotherapy (6,54). Regrettably, the PD-L1 expression status was only available in 9 patients with BMs in our study, and thus we were not able to analysis the predictive role of PD-L1 expression. However, because PD-L1 expression in BMs is different from that in primary lung tumors and sampling for BMs is extremely difficult, the predictive value of PD-L1 expression is actually limited in such patients. Diagnosis-specific graded prognostic assessment (DS-GPA) score is the most widely used prognostic stratification model for BMs. Some studies suggested higher DS-GPA scores were related to improved PFS when treated with ICI (7,15), however, no differences in the ORR nor the PFS based on DS-GPA score stratification were detected in our present study. Therefore, it is necessary to explore potential biomarkers that can predict the efficacy of immunotherapy, especially ICI-based combination therapy for lung cancer patients with BMs. Considering the significant difference in clinical outcome of ICI-based therapy between patients with and without cerebellum metastases, the 6 upregulated miRNAs identified in patients with cerebellum metastases may have potential predictive value to ICI-based therapy, but it needs further investigation.

The limitations of this study are as follows: (I) this study is a retrospective study; (II) the number of patients with BMs and patients with cerebellum metastases were small. Therefore, it was difficult to accurately distinguish whether the cerebellum itself was a poor prognostic factor or whether the prognosis was poor due to its high metastatic tumor burden; (III) we did not analyze the impact of cerebellum metastasis in patient cohort who were treated with only chemotherapy, so it is hard to discriminate whether cerebellum metastasis is an immunotherapy-specific poor prognostic; (IV) only lung adenocarcinoma patients were included in this study, so the results of this study should not be interpreted as an extension of NSCLC.

Conclusions

For lung adenocarcinoma patients, those with BMs have inferior response to ICI-based treatment, but not significantly. Among patients with BM, cerebellum metastasis is associated with an unfavorable outcome of ICI-based therapy, and this may be related to dysregulation of sulfur metabolism.

Acknowledgments

The authors appreciate the academic support from the AME Lung Cancer Collaborative Group.

Funding: This study was supported by the Science and Technology Commission of Shanghai Municipality (No. 19411971100) and the National Natural Science Foundation of China (grant No. 82072568).

Footnote

Reporting Checklist: The authors have completed the

STROBE reporting checklist. Available at https://tlcr.amegroups.com/article/view/10.21037/tlcr-22-260/rc

Data Sharing Statement: Available at https://tlcr.amegroups.com/article/view/10.21037/tlcr-22-260/dss

Conflicts of Interest: All authors have completed the ICMJE uniform disclosure form (available at https://tlcr.amegroups.com/article/view/10.21037/tlcr-22-260/coif). The authors have no conflicts of interest to declare.

Ethical Statement: The authors are accountable for all aspects of the work in ensuring that questions related to the accuracy or integrity of any part of the work are appropriately investigated and resolved. The study was conducted in accordance with the Declaration of Helsinki (as revised in 2013). The study was approved by the Ethics Committee of Shanghai Pulmonary Hospital, Tongji University (No. 201907-0375). Informed consents were obtained from patients whose peripheral blood was collected for further exosome analysis and the other patients were informed by telephone because of the retrospective nature.

References

1. Cagney DN, Martin AM, Catalano PJ, et al. Incidence and prognosis of patients with brain metastases at diagnosis of systemic malignancy: a population-based study. Neuro Oncol 2017;19:1511-21.
2. Waqar SN, Samson PP, Robinson CG, et al. Non-small-cell Lung Cancer With Brain Metastasis at Presentation. Clin Lung Cancer 2018;19:e373-9.
3. Pluim D, Ros W, van Bussel MTJ, et al. Enzyme linked immunosorbent assay for the quantification of nivolumab and pembrolizumab in human serum and cerebrospinal fluid. J Pharm Biomed Anal 2019;164:128-34.
4. Brahmer JR, Rodriguez-Abreu D, Robinson AG, et al. KEYNOTE-024 5-year OS update: First-line (1L) pembrolizumab (pembro) vs platinum-based chemotherapy (chemo) in patients (pts) with metastatic NSCLC and PD-L1 tumour proportion score (TPS) >= 50%. Ann Oncol 2020;31:S1181-S1182.
5. Gadgeel S, Garassino MC, Esteban E, et al. KEYNOTE-189: OS Update and Progression After the Next Line of Therapy (PFS2) with Pembrolizumab plus Chemotherapy for Metastatic Nonsquamous NSCLC. J Thorac Oncol 2019;14:S1153.
6. Mansfield AS, Herbst RS, Castro G Jr, et al. Outcomes with pembrolizumab (pembro) monotherapy in patients (pts) with PD-L1-positive NSCLC with brain metastases: Pooled analysis of KEYNOTE-001,-010,-024, and-042. Ann Oncol 2019;30:604-6.
7. Hendriks LEL, Henon C, Auclin E, et al. Outcome of Patients with Non-Small Cell Lung Cancer and Brain Metastases Treated with Checkpoint Inhibitors. J Thorac Oncol 2019;14:1244-54.
8. Enright TL, Witt JS, Burr AR, et al. Combined Immunotherapy and Stereotactic Radiotherapy Improves Neurologic Outcomes in Patients with Non-small-cell Lung Cancer Brain Metastases. Clin Lung Cancer 2021;22:110-9.
9. El Rassy E, Botticella A, Kattan J, et al. Non-small cell lung cancer brain metastases and the immune system: From brain metastases development to treatment. Cancer Treat Rev 2018;68:69-79.
10. Goldberg SB, Schalper KA, Gettinger SN, et al. Pembrolizumab for management of patients with NSCLC and brain metastases: long-term results and biomarker analysis from a non-randomised, open-label, phase 2 trial. Lancet Oncol 2020;21:655-63.
11. Qiao M, Zhou F, Hou L, et al. Efficacy of immune-checkpoint inhibitors in advanced non-small cell lung cancer patients with different metastases. Ann Transl Med 2021;9:34.
12. Sun L, Davis CW, Hwang WT, et al. Outcomes in Patients With Non-small-cell Lung Cancer With Brain Metastases Treated With Pembrolizumab-based Therapy. Clin Lung Cancer 2021;22:58-66.e3.
13. An N, Jing W, Wang H, et al. Risk factors for brain metastases in patients with non-small-cell lung cancer. Cancer Med 2018;7:6357-64.
14. Lamba N, Kearney RB, Catalano PJ, et al. Population-based estimates of survival among elderly patients with brain metastases. Neuro Oncol 2021;23:661-76.
15. Sperduto PW, Yang TJ, Beal K, et al. Estimating Survival

in Patients With Lung Cancer and Brain Metastases: An Update of the Graded Prognostic Assessment for Lung Cancer Using Molecular Markers (Lung-molGPA). JAMA Oncol 2017;3:827-31.
16. Cacho-Díaz B, Cuapaténcatl LD, Rodríguez JA, et al. Identification of a high-risk group for brain metastases in non-small cell lung cancer patients. J Neurooncol 2021;155:101-6.
17. Karlsson AT, Hjermstad MJ, Omdahl T, et al. Overall survival after initial radiotherapy for brain metastases; a population based study of 2140 patients with non-small cell lung cancer. Acta Oncol 2021;60:1054-60.
18. Vilariño N, Bruna J, Bosch-Barrera J, et al. Immunotherapy in NSCLC patients with brain metastases. Understanding brain tumor microenvironment and dissecting outcomes from immune checkpoint blockade in the clinic. Cancer Treat Rev 2020;89:102067.
19. Seike T, Fujita K, Yamakawa Y, et al. Interaction between lung cancer cells and astrocytes via specific inflammatory cytokines in the microenvironment of brain metastasis. Clin Exp Metastasis 2011;28:13-25.
20. Böttcher C, Schlickeiser S, Sneeboer MAM, et al. Human microglia regional heterogeneity and phenotypes determined by multiplexed single-cell mass cytometry. Nat Neurosci 2019;22:78-90.
21. Irvin DM, McNeill RS, Bash RE, et al. Intrinsic Astrocyte Heterogeneity Influences Tumor Growth in Glioma Mouse Models. Brain Pathol 2017;27:36-50.
22. Henrik Heiland D, Ravi VM, Behringer SP, et al. Tumor-associated reactive astrocytes aid the evolution of immunosuppressive environment in glioblastoma. Nat Commun 2019;10:2541.
23. Böing AN, van der Pol E, Grootemaat AE, et al. Single-step isolation of extracellular vesicles by size-exclusion chromatography. J Extracell Vesicles 2014.
24. Langmead B, Salzberg SL. Fast gapped-read alignment with Bowtie 2. Nat Methods 2012;9:357-9.
25. Kanehisa M, Goto S, Kawashima S, et al. The KEGG resource for deciphering the genome. Nucleic Acids Res 2004;32:D277-80.
26. Mao X, Cai T, Olyarchuk JG, et al. Automated genome annotation and pathway identification using the KEGG Orthology (KO) as a controlled vocabulary. Bioinformatics 2005;21:3787-93.
27. Harshyne LA, Nasca BJ, Kenyon LC, et al. Serum exosomes and cytokines promote a T-helper cell type 2 environment in the peripheral blood of glioblastoma patients. Neuro Oncol 2016;18:206-15.
28. Xing F, Liu Y, Wu SY, et al. Loss of XIST in Breast Cancer Activates MSN-c-Met and Reprograms Microglia via Exosomal miRNA to Promote Brain Metastasis. Cancer Res 2018;78:4316-30.
29. Kim R, Keam B, Kim S, et al. Differences in tumor microenvironments between primary lung tumors and brain metastases in lung cancer patients: therapeutic implications for immune checkpoint inhibitors. BMC Cancer 2019;19:19.
30. Gryglewski G, Seiger R, James GM, et al. Spatial analysis and high resolution mapping of the human whole-brain transcriptome for integrative analysis in neuroimaging. Neuroimage 2018;176:259-67.
31. Kleinridders A, Ferris HA, Reyzer ML, et al. Regional differences in brain glucose metabolism determined by imaging mass spectrometry. Mol Metab 2018;12:113-21.
32. Ayata P, Badimon A, Strasburger HJ, et al. Epigenetic regulation of brain region-specific microglia clearance activity. Nat Neurosci 2018;21:1049-60.
33. Rodrigues G, Hoshino A, Kenific CM, et al. Tumour exosomal CEMIP protein promotes cancer cell colonization in brain metastasis. Nat Cell Biol 2019;21:1403-12.
34. Morad G, Carman CV, Hagedorn EJ, et al. Tumor-derived extracellular vesicles breach the intact blood-brain barrier via transcytosis. ACS Nano 2019;13:13853-65.
35. Arnold J, Schattschneider J, Blechner C, et al. Tubulin Tyrosine Ligase Like 4 (TTLL4) overexpression in breast cancer cells is associated with brain metastasis and alters exosome biogenesis. J Exp Clin Cancer Res 2020;39:205.
36. Fong MY, Zhou W, Liu L, et al. Breast-cancer-secreted miR-122 reprograms glucose metabolism in premetastatic niche to promote metastasis. Nat Cell Biol 2015;17:183-94.
37. Cascone T, McKenzie JA, Mbofung RM, et al. Increased Tumor Glycolysis Characterizes Immune Resistance to Adoptive T Cell Therapy. Cell Metab 2018;27:977-987.e4.
38. Byun JK, Park M, Lee S, et al. Inhibition of Glutamine Utilization Synergizes with Immune Checkpoint Inhibitor to Promote Antitumor Immunity. Mol Cell 2020;80:592-606.e8.
39. Venneti S, Thompson CB. Metabolic Reprogramming in Brain Tumors. Annu Rev Pathol 2017;12:515-45.
40. Ciminera AK, Jandial R, Termini J. Metabolic advantages and vulnerabilities in brain metastases. Clin Exp Metastasis 2017;34:401-10.
41. Liu B, Zhang X. Metabolic Reprogramming Underlying Brain Metastasis of Breast Cancer. Front Mol Biosci 2022;8:791927.

42. Chan KX, Phua SY, Van Breusegem F. Secondary sulfur metabolism in cellular signalling and oxidative stress responses. J Exp Bot 2019;70:4237-50.
43. Miller CG, Schmidt EE. Sulfur Metabolism Under Stress. Antioxid Redox Signal 2020;33:1158-73.
44. Ward NP, DeNicola GM. Sulfur metabolism and its contribution to malignancy. Int Rev Cell Mol Biol 2019;347:39-103.
45. Kumar M, Sandhir R. Hydrogen Sulfide in Physiological and Pathological Mechanisms in Brain. CNS Neurol Disord Drug Targets 2018;17:654-70.
46. Zhang C, Xu J, Chen L, et al. Multi-omics landscape of circadian rhythm pathway alterations in Glioma. Bioengineered 2021;12:3294-308.
47. Blakeman V, Williams JL, Meng QJ, et al. Circadian clocks and breast cancer. Breast Cancer Res 2016;18:89.
48. Parascandolo A, Bonavita R, Astaburuaga R, et al. Effect of naive and cancer-educated fibroblasts on colon cancer cell circadian growth rhythm. Cell Death Dis 2020;11:289.
49. Razi Soofiyani S, Ahangari H, Soleimanian A, et al. The role of circadian genes in the pathogenesis of colorectal cancer. Gene 2021;804:145894.
50. Rahman S, Kraljević Pavelić S, Markova-Car E. Circadian (De)regulation in Head and Neck Squamous Cell Carcinoma. Int J Mol Sci 2019;20:2662.
51. Papagiannakopoulos T, Bauer MR, Davidson SM, et al. Circadian Rhythm Disruption Promotes Lung Tumorigenesis. Cell Metab 2016;24:324-31.
52. Liu C, Li X, Shao H, et al. Identification and Validation of Two Lung Adenocarcinoma-Development Characteristic Gene Sets for Diagnosing Lung Adenocarcinoma and Predicting Prognosis. Front Genet 2020;11:565206.
53. Chen J, Dong X, Lei X, et al. Non-small-cell lung cancer pathological subtype-related gene selection and bioinformatics analysis based on gene expression profiles. Mol Clin Oncol 2018;8:356-61.
54. Spigel DR, Chaft JE, Gettinger S, et al. FIR: Efficacy, Safety, and Biomarker Analysis of a Phase II Open-Label Study of Atezolizumab in PD-L1-Selected Patients With NSCLC. J Thorac Oncol 2018;13:1733-42.

(English Language Editor: J. Teoh)

Cite this article as: Zhou J, Wu Y, Xie M, Fang Y, Zhao J, Lee SY, Im Y, Ye L, Su C. The clinical outcome and risk factors analysis of immune checkpoint inhibitor-based treatment in lung adenocarcinoma patients with brain metastases. Transl Lung Cancer Res 2022;11(4):656-669. doi: 10.21037/tlcr-22-260

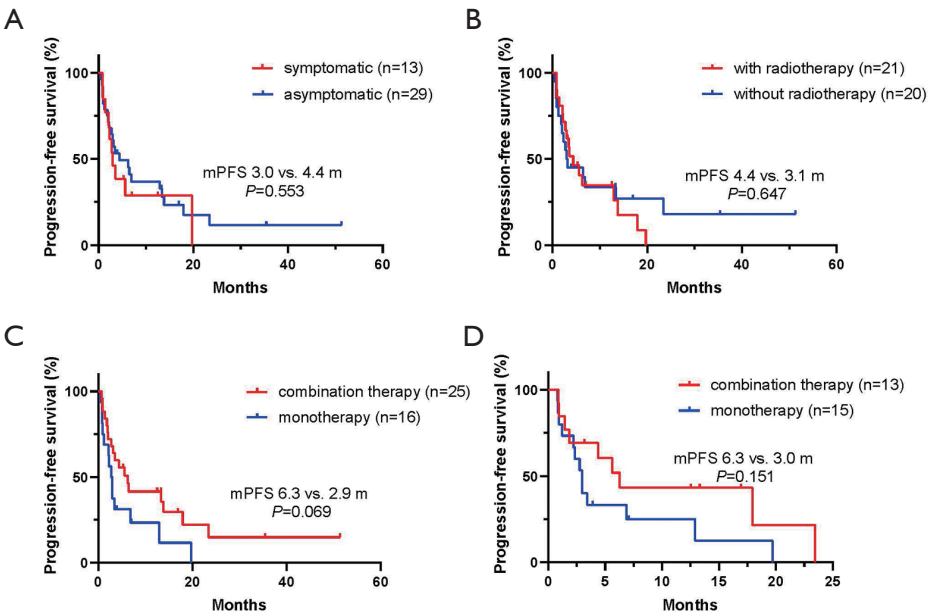

Figure S1 PFS comparison in different subgroups of patients with BMs: patients who presented with or without neurological symptoms (A), patients who had received radiotherapy for intracranial lesion or not (B), patients who were treated with ICI monotherapy or combination therapy (C), patients who were treated with ICI monotherapy or combination therapy at posterior-line (D). PFS, progression-free survival; BMs, brain metastases; ICI, immune checkpoint inhibitor.

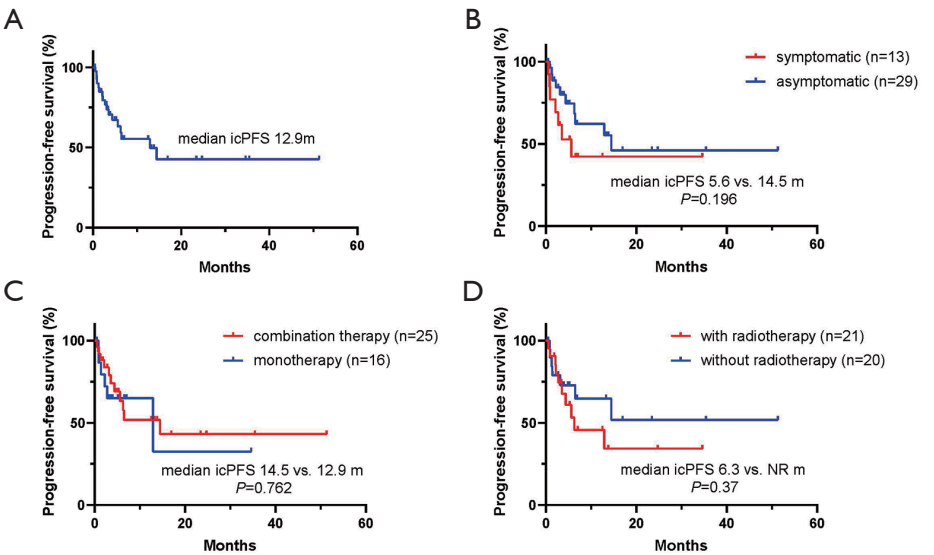

Figure S2 icPFS of all patients with BMs (A). icPFS comparison in different subgroups of patients with BMs: patients who presented with or without neurological symptoms (B), patients who were treated with ICI monotherapy or combination therapy (C), patients who had received radiotherapy for intracranial lesion or not (D). icPFS intracranial progression-free survival; BMs, brain metastases; ICI, immune checkpoint inhibitor.

https://dx.doi.org/10.21037/tlcr-22-260

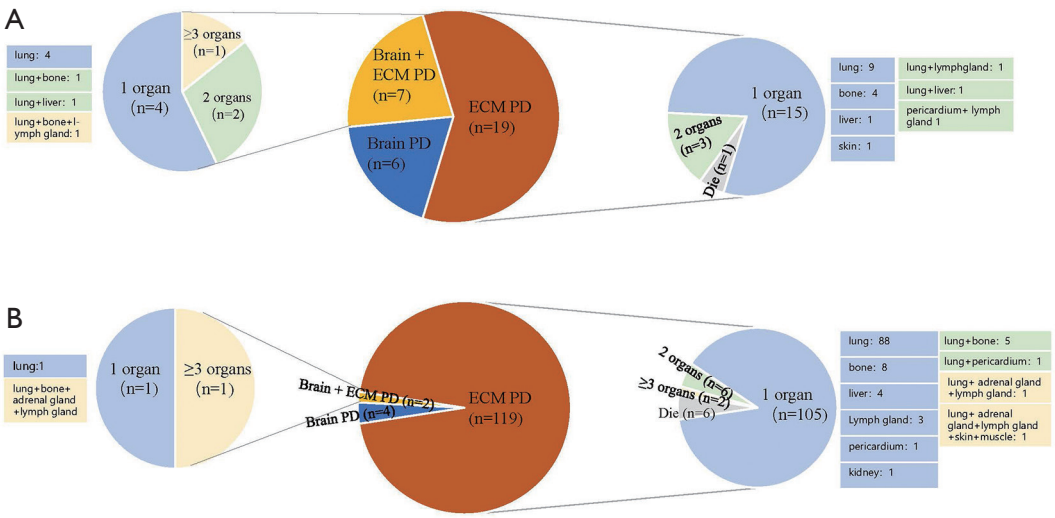

Figure S3 Progression patterns of patients with (A) or without (B) BMs after ICI-based treatment. For patients presented as "ECM PD", the distribution of patients with different number of involved organs was showed in the right pie, and the table aside the pie listed the specific organs involved for each patient. For patients presented as "Brain + ECM PD", the distribution of patients with different number of organs involved in ECM PD was showed in the left pie, and the table aside the pie listed the specific organs for each patient. BMs, brain metastases; ICI, immune checkpoint inhibitor; ECM, extracranial metastases; PD, progression disease.

https://dx.doi.org/10.21037/tlcr-22-260

Table S1 Univariate and multivariate analysis of PFS in patients with BMs

Factor	No. (%)	Univariate analysis			Multivariate analysis	
		PFS	HR (95% CI)	P value	HR (95% CI)	P value
Age, years						
<50	12 (29.3)	2.2	1.747 (0.763–4.002)	0.187		
50–60	13 (31.7)	6.5	0.809 (0.339–1.929)	0.632		
>60	16 (39.0)	4.4	–			
Sex						
Male	29 (70.7)	5.6	0.834 (0.380–1.829)	0.651		
Female	12 (29.3)	3.0	–			
Smoking						
No/light	31 (75.6)	3.0	1.519 (0.655–3.523)	0.330		
Heavy	10 (24.4)	12.9	–			
ECOG						
0–1	31 (75.6)	6.3	0.414 (0.182–0.939)	0.035	0.602 (0.251–1.441)	0.254
2–3	10 (24.4)	2.3	–		–	
ECM						
Present	36 (87.8)	13.8	1.627 (0.562–4.711)	0.369		
Absent	5 (12.2)	3.4	–			
No. of BMs				0.159		
<5	22 (53.7)	4.4	0.382 (0.142–1.028)			
5–10	13 (31.7)	5.6	0.458 (0.162–1.298)			
>10	6 (14.6)	2.8	–			
DS-GPA						
0–1	7 (17.1)	3.4	1.525 (0.506–4.596)	0.454		
1.5–2	25 (61.0)	5.6	0.873 (0.364–2.098)	0.762		
2.5–3.0	9 (21.9)	3.2	–			
Cerebellum Metastasis						
Yes	20 (48.8)	2.8	2.948 (1.326–6.556)	0.008	2.552 (1.128–5.772)	0.024
No	21 (51.2)	13.8	–		–	
Neurological symptom						
Yes	13 (31.7)	3.0	1.259 (0.587–2.696)	0.554		
No	28 (68.3)	4.4	–			
Radiotherapy						
Yes	21 (51.2)	4.4	1.181 (0.578–2.416)	0.648		
No	20 (48.8)	3.0	–			
ICI Line						
1	13 (31.7)	3.5	0.828 (0.388–1.765)	0.625		
≥2	28 (68.3)	3.4	–			
Treatment regimen						
Mono	16 (39.0)	2.8	1.925 (0.938–3.948)	0.074	1.518 (0.702–3.283)	0.289
Combination	25 (61.0)	6.3	–		–	

Factors with P value <0.1 in univariate analysis were included to multivariate analysis, but "No. of BMs" was excluded causing collinearity with "Cerebellum Metastasis". PFS, progression-free survival; ECOG, Eastern Cooperative Oncology Group; ECM, extracranial metastases; BMs, brain metastases; DS-GPA, diagnosis-specific graded prognostic assessment; ICI, immune checkpoint inhibitor; Mono, monotherapy.

https://dx.doi.org/10.21037/tlcr-22-260

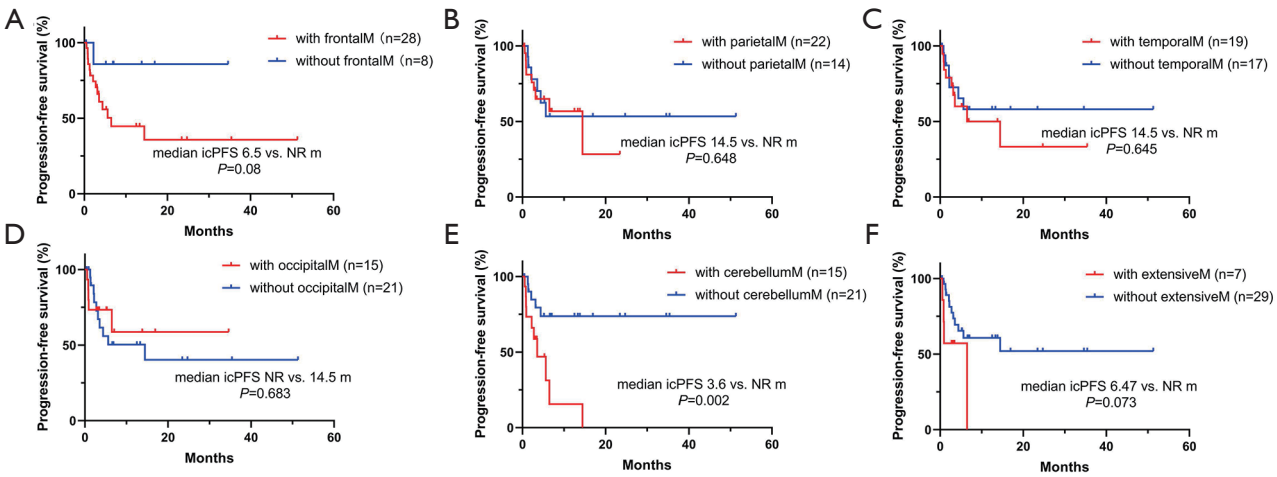

Figure S4 icPFS comparison between patients with or without different region metastases: frontal lobe (A), parietal lobe (B), temporal lobe (C), occipital lobe (D), cerebellum (E), and concurrent the above five regions (F). icPFS intracranial progression-free survival.

Table S2 List of target genes predicted from the upregulated miRNAs in patients with cerebellum metastasis, compared with those without

KANSL2	*BCAN*	*RAB38*	*TSSC4*	*BHLHE40*	*ARHGEF19*
TCTN2	*AURKA*	*BORCS5*	*GTF3A*	*TMEM250*	*TSEN2*
MYO15A	*FYCO1*	*COL16A1*	*COL16A1*	*MAEL*	*DPYSL2*
RPP25	*HIP1R*	*AGBL5*	*TCTN2*	*CFAP99*	*PAPSS1*
RPUSD2	*ADAMTSL5*	*BLACAT1*	*AKR1E2*	*GOLM1*	

https://dx.doi.org/10.21037/tlcr-22-260